



Deposited via The University of Leeds.

White Rose Research Online URL for this paper:

<https://eprints.whiterose.ac.uk/id/eprint/180563/>

Version: Accepted Version

Article:

Zhai, X, Wang, X, Zhang, J et al. (2020) Extruded low density polyethylene-curcumin film: A hydrophobic ammonia sensor for intelligent food packaging. *Food Packaging and Shelf Life*, 26. 100595. ISSN: 2214-2894

<https://doi.org/10.1016/j.fpsl.2020.100595>

© 2020 Elsevier Ltd. All rights reserved. This manuscript version is made available under the CC-BY-NC-ND 4.0 license <http://creativecommons.org/licenses/by-nc-nd/4.0/>.

Reuse

This article is distributed under the terms of the Creative Commons Attribution-NonCommercial-NoDerivs (CC BY-NC-ND) licence. This licence only allows you to download this work and share it with others as long as you credit the authors, but you can't change the article in any way or use it commercially. More information and the full terms of the licence here: <https://creativecommons.org/licenses/>

Takedown

If you consider content in White Rose Research Online to be in breach of UK law, please notify us by emailing eprints@whiterose.ac.uk including the URL of the record and the reason for the withdrawal request.

10 **Abstract**

11 A hydrophobic film was developed using low density polyethylene (LDPE) and
12 curcumin with the melting extrusion method. The hydrophobic nature of the LDPE
13 endowed the film with good stability to pH buffer solutions, namely without obvious
14 color change or curcumin leaching, when immersed in pH buffer solutions. The LDPE-
15 curcumin composite film was sensitive to ammonia (NH₃), and the limit of detection
16 (LOD) of LDPE-curcumin film to NH₃ at 90% RH was 0.18 μM. When the LDPE-
17 curcumin film was used to monitor beef and silver carp spoilage at 4 °C, it showed light
18 yellow-to-light brown color changes along with the storage time, resulting from the
19 increasing TVB-N contents of the meat samples. As the developed LDPE-curcumin
20 film was totally non-toxic and suitable for industrial production in a large scale, there
21 will be a good potential for its application in intelligent food packaging.

22 **Keywords**

23 Hydrophobic film; low density polyethylene; curcumin; meat spoilage; intelligent
24 packaging

25 **1. Introduction**

26 Intelligent food packaging has received great attention in modern food industry. It
27 particularly aims to *in-situ* and real-time monitor the food quality in individual
28 packages for food quality assessment and safety assurance. To date, various
29 colorimetric sensors (Lin, et al., 2016; Long, et al., 2019; Zhai, et al., 2019) and
30 indicators (Saliu & Della Pergola, 2018; Wang, Lu, & Gunasekaran, 2017; C. Zhang,
31 et al., 2013), and wireless electronic sensors (Koskela, et al., 2015; Z. Ma, et al., 2018;
32 Zhu, Desroches, Yoon, & Swager, 2017) have been developed for intelligent packaging,
33 with advantages of good portability, low cost, and easy fabrication. Among them,
34 colorimetric sensors have been widely studied, because their color changes can be
35 directly assessed by naked eye or using digital imaging technology.

36 Meat spoilage during distribution can easily occur, due to enzymatic reaction and
37 microbial contamination. Total volatile basic amines (TVB-N), such as trimethylamines,
38 dimethylamines and ammonia, are widely regarded as a meat spoilage indicator. To
39 achieve the real-time evaluation of meat spoilage, a number of studies have tried to use
40 synthetic pH-sensitive dyes to develop the TVB-N sensors in intelligent packaging
41 systems (Chun, Kim, & Shin, 2014; Domínguez-Aragón, Olmedo-Martínez, &
42 Zaragoza-Contreras, 2018; Mo, et al., 2017; A. Pacquit, et al., 2006). Traditionally,
43 considering of the potential toxicity of the synthetic dyes, pH-sensitive dyes are
44 generally encapsulated into a polymer and then covered by a gas-permeable and ion-
45 impermeable membrane (GPM) to prevent the leaching of synthetic dyes from the films
46 to the humid food packaging environment (Kuswandi, et al., 2012; K. Lee, Baek, Kim,
47 & Seo, 2019; Wells, Yusufu, & Mills, 2019). Of late, chemical covalent cross-linking
48 (Jia, et al., 2019) and melting extrusion methods (Wells, et al., 2019) have also been
49 proposed to embed the pH-sensitive dyes into solid films and simultaneously prevent
50 the leaching of dyes, which provided new approaches to design colorimetric films for
51 intelligent food packaging.

52 Although the synthetic pH-sensitive dyes showed good performance in developing
53 meat quality indicators, it is still highly desirable to develop totally safe colorimetric

54 films (S. J. Lee & Rahman, 2014). In recent years, natural edible pigments, such as
55 anthocyanins (Dudnyk, Janeček, Vaucher-Joset, & Stellacci, 2018; Q. Ma & Wang,
56 2016; Zhai, et al., 2018; J. Zhang, et al., 2019), alizarin (Ezati, Tajik, & Moradi, 2019),
57 betalains (Qin, Liu, Zhang, & Liu, 2020) and curcumin (Kuswandi, Jayus, Larasati,
58 Abdullah, & Heng, 2011; Liu, et al., 2018; Q. Ma, Du, & Wang, 2017), have been used
59 to develop pH-sensitive films to monitor meat quality. These pigments are generally
60 embedded in hydrophilic polymer films, such as chitosan (X. Zhang, Lu, & Chen, 2014),
61 gelatin (Chayavanich, Thiraphibundet, & Imyim, 2019), κ -carrageenan (Liu, et al.,
62 2019), polyvinyl alcohol (Qin, et al., 2020) and so forth. However, the big concern is
63 that the package with fresh meat has high relative humidity (RH), so that the hydrophilic
64 polymer film could inevitably absorb water from the internal package environment,
65 which induced the leaching of pigments from the film (Liu, et al., 2019; Liu, et al., 2018;
66 Q. Ma, et al., 2017; Zhai, et al., 2020). Even though the leaching of natural pigments
67 would not lead to food safety issues, it should have great effect on the indicating
68 property of the film due to the unpredictable fluctuation of pigment content in the film
69 caused by leaching (S. Huang, et al., 2019; Q. Ma, et al., 2017; Zhai, et al., 2017).
70 Furthermore, the sensing ability of the hydrophilic films to volatile gases may be
71 susceptible to the humidity of the package environment (Zhai, et al., 2020). Hence,
72 there is an urgent need to reduce the leaching of the natural pigments and the effect of
73 humidity on the sensing ability of the film.

74 To meet this requirement, in this study, we tried to develop a hydrophobic
75 colorimetric film by incorporating natural pigment curcumin in LDPE using the melting
76 extrusion method. On one hand, curcumin is a low molecular-weight phenolic
77 compound obtainable from the rhizomes of turmeric (*Curcuma longa* Linn.), and has
78 been widely used as a food coloring agent owing to its intense yellow color (Xiang,
79 Sun-Waterhouse, Cui, Wang, & Dong, 2018). On the other hand, LDPE is a nontoxic
80 polymer and LDPE films have been widely used in food packaging due to its good
81 mechanical and water barrier properties. A recent study has shown the feasibility of
82 developing LDPE-curcumin films by using the melting extrusion method (Zia, Paul,

83 Heredia-Guerrero, Athanassiou, & Fragouli, 2019). However, to our best knowledge,
84 the indicating property of the LDPE-curcumin film, as a colorimetric gas sensor, for
85 intelligent food packaging has not been reported yet. The experimental results showed
86 that the LDPE-curcumin film could prevent the leaching of curcumin in buffer solutions.
87 Meanwhile, the film was sensitive to NH₃ and could exhibit visible color changes when
88 used to monitor meat spoilage. As the LDPE-curcumin film is nontoxic, cost effective
89 and fabricated by using the melting extrusion method (Fig. S1), a classical polymer
90 technological process for large scale industrial production, it presented a promising
91 method to develop natural pigment based colorimetric films for intelligent packaging.

92 **2. Materials and methods**

93 2.1. Materials and reagents

94 Fresh beef and live silver carp were bought from a local market (Zhenjiang, China).
95 LDPE powder was purchased from Shanghai Jiexun Plasticizing Co., Ltd. (Shanghai,
96 China). Curcumin, magnesium chloride, magnesium nitrate, sodium chloride,
97 potassium sulphate, citric acid, sodium citrate, hydrochloric acid, sodium hydroxide,
98 methyl red, methylene blue, and boric acid were purchased from Sinopharm Chemical
99 Reagent Co., Ltd (Shanghai, China). Gaseous NH₃ was purchased from Thorpe
100 Chemical Co., Ltd (Zhenjiang, China).

101 2.2. Preparation of the LDPE-curcumin film

102 The preparation of LDPE-curcumin film was according to a previous literature with
103 slight modification (Zia, et al., 2019). First, 1 g of curcumin powder and 100 g of LDPE
104 powder were mixed by mechanical stirring. The curcumin-covered LDPE powder was
105 then pelletised using a twinscrew extruder (Baopin International Precision Instruments
106 Co., Ltd.) with screws of 20 mm diameter, and length to diameter ratio of 40. The
107 operating temperatures were set at 90, 110, 120, 130 and 130 °C for the feeding, heating
108 zones 1-3 and pelletising die, respectively. The extruder screw speed was 80 rpm
109 throughout the extrusion process. The obtained LDPE-curcumin pellets were then
110 extruded into a thin, clear yellow-colored plastic film with operating temperatures of
111 130 °C, using a single-screw extruder (Baopin International Precision Instruments Co.,

112 Ltd.) with a screw of 20 mm diameter and length to diameter ratio of 28. The thickness
113 of the obtained film was $\sim 50 \mu\text{m}$. The control LDPE film without curcumin was also
114 prepared following the same procedures.

115 2.3. Response to pH buffer solutions

116 The pH buffer solutions in the range of 2-12 were prepared by using 0.2 M disodium
117 hydrogen phosphate, 0.2 M citric acid and 0.2 M sodium hydroxide solutions with
118 different proportions. Curcumin powder was added to the prepared pH buffer solutions
119 with the addition of 20% ethanol as curcumin has an extremely low solubility. Then,
120 the UV-Vis spectra of curcumin solutions were recorded. The release of curcumin from
121 the film to buffer solutions was investigated by immersing 4 g of LDPE-curcumin film
122 in 100 mL of the buffer solution at $25 \text{ }^\circ\text{C}$. The film was taken out from the buffer
123 solution after every 24 h, and the UV-Vis spectra of the solutions were recorded.

124 2.4. Response to NH_3 under different RH

125 First, the LDPE-curcumin film ($30 \times 10 \text{ mm}$) was adhered on the inner surface of the
126 cuvette. The cuvettes were put in desiccators with silica gels, NaBr saturated solution
127 and Na_2HPO_4 saturated solution for 24 h at $25 \text{ }^\circ\text{C}$. The actual RH in the desiccators
128 were determined to be 6% (silica gels), 55% (NaBr saturated solution), and 95%
129 (Na_2HPO_4 saturated solution), by using a commercial hygrometer (AR837, SMART
130 SENSOR). The cuvettes were sealed with rubber caps before they were taken out from
131 the desiccators. A certain amount of NH_3 was injected into the cuvettes by using needle
132 syringes. Here, the concentration of NH_3 was determined by trapping NH_3 with 10 mL
133 2% aqueous solution of boric acid and 3 droplets of mixed indicator produced from
134 dissolution of 0.2 g of methyl red and 0.1 g of methylene blue to 100 mL of ethanol.
135 After that, the boric acid solution was titrated with a 0.01 M hydrochloric acid solution,
136 and NH_3 was quantified by the hydrochloric acid used.

137 The reversibility of the film when reacting with NH_3 was also investigated (Khattab,
138 Dacrory, Abou-Yousef, & Kamel, 2019). The film was first reacted with $80 \mu\text{M}$ NH_3
139 under 90% RH for 30 min, and then was put in air for 1 h at $25 \text{ }^\circ\text{C}$. The UV-vis spectra
140 of the film before reacting with NH_3 , after reacting with NH_3 , and after recovering in

141 air were detected. This process was repeated for 5 times.

142 2.5. Stability test of the film at different temperatures

143 The film (30 × 10 mm) was adhered on the inner surface of the cuvette. The cuvette
144 was placed in a constant temperature and humidity incubator with a fluorescent lamp.
145 The absorbance at 420 nm of the LDPE-curcumin film was recorded by using the UV-
146 Vis spectrometer.

147 2.6. Application of the film in monitoring meat spoilage

148 Live silver carp was pretreated by removing its innards, head, tail and feathers. Then,
149 it was cleaned by water and diced. A quantity of 500 g of diced fresh beef and silver
150 carp were put into a polyethylene terephthalate (PET) box with a buttoned lid. The
151 dimensions of the box is 165 × 115 × 43 mm (L × W × H). The LDPE-curcumin film
152 was cut to square (20 × 20 mm) and was put in the headspace of the box. The
153 experimental setup was according a previous studies (Chun, et al., 2014; Alexis Pacquit,
154 et al., 2007). As the LDPE-curcumin film is transparent, which is not good for *in-situ*
155 color measurement, it was put on a white cellulose acetate filter paper (25 × 25 mm)
156 that served as a background. Then, the filter paper was tightly adhered onto the internal
157 surface of the PET lid by using adhesive tape (see Fig. S4). The above processes were
158 conducted in a clean bench. Finally, the PET boxes were placed in an incubator at 4 °C
159 in a refrigerator. The color parameters of the films were detected by using a portable
160 colorimeter (CM-2300d, Konica Minolta, Inc., Japan). The chromatic parameters of ΔE
161 and ΔC^* were calculated according to following equations:

$$162 \quad \Delta E = \sqrt{(L_t^* - L_0^*)^2 + (a_t^* - a_0^*)^2 + (b_t^* - b_0^*)^2} \quad (1)$$

$$163 \quad \Delta C^* = \sqrt{(a_t^* - a_0^*)^2 + (b_t^* - b_0^*)^2} \quad (2)$$

164 where L_t^* , a_t^* and b_t^* were the color parameters of the LDPE-curcumin film after a
165 certain storage time, and L_0^* , a_0^* and b_0^* were the initial color parameters of the LDPE-
166 curcumin film.

167 The total volatile basic nitrogen (TVB-N) content of meat samples was measured
168 according to a previous literature (Cai, Chen, Wan, & Zhao, 2011), following the

169 Chinese Standard (GB 5009. 228-2016). Briefly, 20 g of meat sample was put in a
170 beaker with 100 mL of distilled water, and then crushed by using a tissue homogenizer.
171 The homogenate was filtered with filter papers to obtain the filtrate. Then, 10 mL of
172 filtrate was transferred to a Kjeldahl distillation unit. The volatile biogenic amines were
173 distilled, and the distillate was collected with 10 mL of boric acid solution (20 g/L)
174 containing 5 droplets of mixed indicator that was made by dissolving 0.2 g of methyl
175 red and 0.1 g methylene blue in 300 mL ethanol. Finally, the distillate was titrated with
176 0.01 M HCl solution. The TVB-N content was calculated according to the amount of
177 HCl used during titration, and expressed as mg/100 g.

178 The total viable counts (TVC) of meat samples were measured using the Plate Count
179 Agar (Mehdizadeh, Tajik, Langroodi, Molaei, & Mahmoudian, 2020). Meat samples
180 (25 g) were added to 225 mL of phosphate buffer solution (PBS), and then homogenized
181 by using a homogenizer (IKA, Germany). The homogeneous solution was then serially
182 diluted at a ratio of ten (V/V) by using the PBS. 1 mL of the diluted solution was spread
183 on the surface of the plate count agar medium in Petri dishes, which were further
184 incubated at 35 °C for 2 days. The bacterial counts were expressed as colony-forming
185 units (CFU) per gram of meat sample and then transformed to base 10 logarithm values,
186 namely $\log_{10}(\text{CFU/g})$.

187 2.7. Statistical analysis

188 All the experiments were conducted in triplicate and the data was expressed as means
189 \pm standard deviation.

190 3. Result and discussion

191 3.1. Stability of curcumin during extrusion process

192 In this work, curcumin was embedded into LDPE through extruding method, during
193 which LDPE powder was heated (≤ 130 °C) to molten state and to mix with curcumin.
194 Therefore, the stability of curcumin under heating should be investigated. The curcumin
195 powder was first heated in oven in air, and then exposed to NH_3 . As shown in Fig. 1,
196 the curcumin powder did not show obvious color changes after 1 h heating at 130 °C,
197 but exhibited yellow-to-brown color changes when subsequently reacted with NH_3 .

198 This result indicated that the curcumin powder maintained its sensitivity to NH₃ after
199 being heated under 130 °C for 1 h in air. However, it presented yellow-to-dark brown
200 color change when heated at 180 °C for 1 h, while did not show obvious color changes
201 exposing to NH₃. This can be due to that the curcumin powder was intensely oxidized
202 and decomposed to ferulic acid and 4-vinyl guaiacol under 180 °C (Esatbeyoglu,
203 Ulbrich, Rehberg, Rohn, & Rimbach, 2015), and therefore lost the reactivity with NH₃.
204 Hence, the melting temperature (≤ 130 °C) during the extruding process would not
205 significantly induce the oxidative decomposition of curcumin. In addition, the
206 pelletizing process was conducted in vacuum condition, which can prevent curcumin
207 from being oxidized. As shown in Fig. 1, the LDPE-curcumin film presented a light
208 yellow color, and turned to light brown in response to NH₃, indicating its sensing ability
209 to NH₃. Furthermore, the incorporation of curcumin had no significant effect on the
210 microstructure of LDPE film. As shown in Fig. S2, the LDPE-curcumin film had a
211 dense cross section similar to that of the LDPE film. No big particle agglomerates, air
212 gaps, cracks, or detachment zones were evident, which was in line with a previous study
213 (Zia, et al., 2019). These results indicated that curcumin, as a natural pigment, can be
214 embedded into LDPE through extruding technology, and the fabricated LDPE-
215 curcumin film was sensitive to NH₃.

216 3.2. Response of curcumin and LDPE-curcumin film to pH buffer solutions

217 As mentioned, the package with fresh meat generally has high RH, and the volatile
218 water vapor would be adsorbed on the surface of the film fixed on the headspace of the
219 packages. As a result, some non-neutral gases, such as volatile amines (primary and
220 secondary amines), carbon dioxide and hydrogen sulfide, generated from meats would
221 partially dissolve and then hydrolyze or ionize in the adsorbent water before they
222 directly diffused into the films. This would therefore make the film exposed to a non-
223 neutral aqueous microenvironment. Therefore, the stability of the LDPE-curcumin film
224 in pH buffer solutions which simulated the non-neutral aqueous microenvironment was
225 investigated.

226 Firstly, the colors and UV-Vis spectra of curcumin solutions were investigated, as

227 shown in Fig. 2. Curcumin solution showed nearly the same yellow color at pH 2-8,
228 while turned to brown at pH 9-10 and then reddish brown at pH 11-12 (Fig. 2A), which
229 was line with a previous study (Pourreza & Golmohammadi, 2015). Correspondingly,
230 the UV-Vis spectra of curcumin solution showed a maximum absorption peak at nearly
231 420 nm at pH 2-8, and the absorbance values slightly decreased with the increase of pH
232 (Fig. 2B). When pH increased from 9 to 12, the maximum absorption peak gradually
233 shifted to 474 nm, and simultaneously the absorbance values rose. The color and
234 spectral changes of curcumin solutions with the increase of pH was due to the
235 deprotonation of curcumin molecular, as described in previous studies (Kotha & Luthria,
236 2019; Liu, et al., 2018; Priyadarsini, 2014).

237 However, the LDPE-curcumin film did not show color changes even being immersed
238 in pH buffer solutions for 6 h (Fig. 2C). This insensitivity of LDPE-curcumin film to
239 pH buffer solutions was further confirmed by the UV-Vis spectra. As shown in Fig. 2D,
240 the LDPE-curcumin films showed nearly the same spectra at pH 2-12, and the range
241 value of the maximum absorbance at 420 nm (A_{420}) was lower than 0.01 (Fig. 2D inset).
242 The L^* , a^* and b^* values of the film were shown in Table S2, indicating no significant
243 difference between the colors of the films. These results could be due to that curcumin
244 was embedded in LDPE molecular to reduce the contact between curcumin and water
245 molecular. Similar phenomenon was also found in an extruded LDPE-bromophenol
246 blue film (Wells, et al., 2019). Apart from this, the presence of curcumin could also
247 reduce the water permeability of LDPE film (Zia, et al., 2019), which could also reduce
248 the contact between curcumin and water.

249 To further investigate the stability of the LDPE-curcumin film in pH buffer solutions,
250 the LDPE-curcumin film was immersed into buffer solutions for 5 d, and the UV-Vis
251 spectra of the lixiviums were determined every day. Fig. 2E shows the photo of
252 lixiviums of the LDPE-curcumin films at the 5th d. The lixiviums were nearly colorless
253 and transparent at pH 2-10, but showed weak yellow at pH 11-12. The corresponding
254 A_{420} values of the lixiviums were shown in Fig. 2F. All the lixiviums showed low A_{420}
255 values that were below 0.03 with weak fluctuations within 5 d, indicating the low

256 curcumin contents in the lixiviums. The slightly higher A_{420} values at pH 11 and 12
257 might be due to the better solubility of curcumin at basic condition (Priyadarsini, 2014).
258 In addition, the color of the LDPE-curcumin film remained yellow at the 5th d, even at
259 pH 11 and 12 (Fig. 2F inset). These results indicated that the leaching of curcumin from
260 the LDPE-curcumin to the pH solution was extremely low.

261 3.3. Response of LDPE-curcumin film to NH₃ under different relative humidity

262 The response of LDPE-curcumin film to NH₃ under different relative humidity (RH)
263 was shown in Fig. 3A. The films turned from light yellow to brown after exposed to
264 NH₃ at 6%, 55% and 95% RH (Fig. 3A inset). The corresponding UV-Vis spectra
265 showed that the maximum absorption peak shifted from ~ 420 nm to ~ 460 nm. It can
266 be also seen that a relative lower RH is good for the reaction between LDPE-curcumin
267 film and NH₃, as LDPE-curcumin showed a deeper brown color and higher absorbance
268 value at ~ 460 nm after exposed to NH₃ under 6% RH than 55% RH, and followed by
269 95% RH.

270 As mentioned above, the LDPE-curcumin film was insensitive to pH buffer solutions,
271 but sensitive to NH₃. These results indicated that the reaction between curcumin and
272 NH₃ is a solid-gas interaction. Although this does not exclude the possibility of there
273 being some water present, the water content is likely to be very small (Mills, Wild, &
274 Chang, 1995). The proposed reaction mechanism was shown in Fig. 3B. The diketo
275 group of curcumin could exhibit keto-enol tautomerism, and the enal form contains
276 three labile protons (Priyadarsini, 2014). When NH₃ diffused into the LDPE-curcumin
277 film (Karim, Hijaz, Kastner, & Smith, 2011; Wells, et al., 2019), it could make the
278 deprotonation of these three active groups of curcumin, and thus inducing the color and
279 the spectral changes. This reaction could be described as Equations 3 and 4 (Mills, et
280 al., 1995). Hence, the reason that a lower RH contributed to the reaction between
281 LDPE-curcumin film and NH₃ may be that more NH₃ molecular had dissolved into
282 water under a higher RH to form NH₃·H₂O, and then was ionized into NH₄⁺ and OH⁻,
283 while the OH⁻ in water drop could not easily diffuse into the film and make the color
284 changes of curcumin.



287 where $\text{NH}_3(\text{g})$ is the gaseous ammonia, K_H is Henry's constant for gaseous ammonia in
288 the plastic film. $\text{NH}_3(\text{dis})$ is the gaseous ammonia dissolved in the plastic film. HR is
289 the protonated form of curcumin. K_1 is an ion-pair formation constant (which depends
290 strongly upon the dissociation equilibrium constant, K_a , of curcumin) and NH_4^+R^- is
291 the ion-pair formed between the dissolved ammonia and HR.

292 The effect of humidity on the hydrophobicity LDPE-curcumin film was quite
293 different from the hydrophilic films incorporated with curcumin that were reported in
294 recent studies (Liu, et al., 2018; Q. Ma, et al., 2017), where it was proposed that NH_3
295 firstly combined with H_2O in the hydrophilic films or the environment surrounding the
296 films, and then the ionized OH^- induced the color change of curcumin. As a result, the
297 higher RH was beneficial to the generation of more OH^- , accelerating the color change
298 of the hydrophilic films (Q. Ma, et al., 2017). However, the reaction mechanism
299 between NH_3 and curcumin in the presence or absence of water may need to be further
300 investigated.

301 3.4. Sensitivity of the film to NH_3

302 The sensitivity of the film to NH_3 was determined at 90% RH, because the packages
303 containing fresh meats (with water coefficients ~ 0.99) generally have high RH. Fig.
304 4A shows the UV-Vis spectra of the film in response to increasing contents of NH_3 . The
305 maximum absorption peak gradually shifted from ~ 420 nm to ~ 474 nm, which was
306 consistent with the changes of UV-Vis spectra of curcumin solutions with increasing
307 pH (see section 3.2). The maximum absorbance value at 420 nm showed a continuous
308 decrease while the absorbance value at 540 nm increased, with the increase of NH_3
309 concentration. Generally, visible color absorbs light of wavelengths corresponding to
310 its complementary color (Choi, Lee, Lacroix, & Han, 2017). Yellow color absorbs light
311 of wavelength corresponding to its complementary color, blue (~ 400 - 480 nm), and red
312 color absorbs light of the wavelength corresponding to its complementary color, green

313 (~ 495-570 nm). Hence, the absorbance ratio at 540 nm versus 420 nm (A_{540}/A_{420}),
314 wavelength of each complementary color, could indicate the increase of red color
315 intensity compared to yellow color intensity, with a deeper red color when A_{540}/A_{420}
316 value was high. As shown in Fig. 4B, the A_{540}/A_{420} value increased with the NH_3
317 concentration, indicating that the color of the film gradually presented a yellow-to-red
318 transition. In addition, the calibration curves showed that the A_{540}/A_{420} value had good
319 linear relationship with the NH_3 concentration in the range of 0-80 μM and 100-240
320 μM , with R^2 of 0.9906 and 0.9897, respectively. Accordingly, the limit of detection
321 (LOD) of the LDPE-curcumin film to NH_3 was determined to be 0.18 μM , by using
322 Equation 5 (Courbat, Briand, Damon-Lacoste, Wöllenstein, & de Rooij, 2009):

$$323 \quad LOD = \frac{3K}{N} \quad (5)$$

324 where K is the standard deviation of blank measurements and N is slope of the
325 calibration curve (0.9906).

326 The LOD of LDPE-curcumin film was comparable to that of some other colorimetric
327 sensors (see Table S2). It is generally expected that the sensing film could have high
328 sensitivity to NH_3 . There are several key factors of the pigments (or dyes) based
329 colorimetric film that determine the sensitivity: (1) The acid dissociation constant ($\text{p}K_a$)
330 value of a pigment. Generally, a lower $\text{p}K_a$ of the pigment is good for its color change
331 (Mills, et al., 1995). (2) The content of pigments. A relatively lower content of pigment
332 in the film was conducive to the sensitivity (Zhai, et al., 2017). (3) The microstructure
333 of the film. For example, porous structure generally could improve the sensitivity
334 because it could provide much more contact areas between the pigments and target
335 gases (Luo & Lim, 2020). However, it should be noted that when more attention have
336 been paid to improving the sensitivity of the films, their stabilities (e.g. under oxygen
337 and high RH environment during storage and usage) ought to be considered at the same
338 time.

339 The response of the film to NH_3 was reversible, namely the film could recover its
340 color after it was separated from NH_3 . As shown in Fig. S3, the initial A_{540}/A_{420} value

341 of the LDPE-curcumin film was 0.4232, while it increased to 0.7302 after reacting with
342 NH_3 for the first time. Then, the A_{540}/A_{420} value decreased to 0.4203 when the film was
343 separated from NH_3 and put in air for 1 h. This meant that the film could almost recover
344 to its original color. This reaction cycle was repeated for 5 times. Finally, when the film
345 was reacted with NH_3 and then recovered in air, the A_{540}/A_{420} values were 0.7172 and
346 0.4343, respectively, which were close to A_{540}/A_{420} values of the first reaction cycle.
347 Hence, the response of the film to NH_3 was reversible.

348 3.5. Stability of the film during storage

349 A good stability for a colorimetric film during storage is important. The A_{420} values
350 of the LDPE-curcumin film stored under visible light along with time were shown in
351 Fig. 5. The A_{420} value of the film showed gradual decrease with storage at 4, 25 and
352 37 °C. This instability of the film could be due to the photodecomposition by loss of
353 two hydrogen atoms from the curcumin molecule, according to a previous study
354 (Tønnesen, Karlsen, & van Henegouwen, 1986). It was obvious that a lower storage
355 temperature was conducive to the stability of the film. The A_{420} values decreased by
356 4.2%, 7.3% and 15.3% after respectively stored at 4, 25 and 37 °C for 16 d. Hence, the
357 LDPE-curcumin film was better to be stored or used at a low temperature to reduce its
358 decomposition.

359 3.6. Application of films in monitoring meat spoilage

360 The LDPE-curcumin film was used to monitor silver carp and beef spoilage in a PET
361 box, as shown in Fig. 6A and 6B, respectively. The color of the LDPE-curcumin film
362 was shown in Table S3. The initial L^* of the film was 86.89, which decreased to 68.96
363 after 1 day storage of silver carp, while a^* and b^* did not significantly change. Similar
364 phenomenon was also observed from the film used for beef. This was because the filter
365 paper and the LDPE-curcumin film were wetted by water vapor, leading to a decrease
366 of light of the film. For both the silver carp and beef packaging, the corresponding a^*
367 value of the LDPE-curcumin film increased, while the b^* value decreased, indicating a
368 gradually stronger red color and a weaker yellow color. Hence, the chromatic parameter
369 ΔC^* , which depends on the changes of a^* and b^* , was used to describe the color changes

370 of the film. It can be seen that the ΔC^* values of the film used for silver carp gradually
371 increased from 0 to 8.25 after storage for 7 days. Meanwhile, the TVB-N value of silver
372 carp increased from 5.95 to 29.31 mg/100 g. Similarly, the ΔC^* values of the film used
373 for beef gradually increased from 0 to 8.25 after storage for 7 days as well, and the
374 TVB-N value of beef increased from 6.34 to 26.21 mg/100 g. The increase of TVB-N
375 with storage time for silver carp and beef was in line with previous studies (Ezati, et al.,
376 2019; Kachele, Zhang, Gao, & Adhikari, 2017). These results indicated that the LDPE-
377 curcumin film could present a yellow-to-brown color change resulting from reacting
378 with the volatile amines of the meats.

379 According to Chinese Standard GB 2707-2016, the rejection limits of TVB-N are 20
380 and 15 mg/100 g for silver carp and beef, respectively. In this study, the TVB-N value
381 of silver carp increased to 20 mg/100 g at nearly 5.3 d, when the ΔC^* value of the film
382 was nearly 3.5 (Fig. 6C). This indicated that if the ΔC^* value of the film was higher
383 than 3.5, then the silver carp sample should not be consumed. Similarly, the TVB-N
384 value of beef sample rose to 15 mg/100 g at nearly 4.2 d, when the ΔC^* of the film was
385 nearly 2.2 (Fig. 6D), indicating that the beef sample should be discarded at this point.

386 TVC is generally used to evaluate the meat spoilage as well (L. Huang, Zhao, Chen,
387 & Zhang, 2013). The TVC of silver carp and beef during storage at 4 °C was shown in
388 Table S3. The TVC of silver carp and beef increased respectively from 3.31 to 9.65
389 $\log_{10}(\text{CFU/g})$, and from 3.55 to 9.49 $\log_{10}(\text{CFU/g})$. Similar outcomes have been found
390 in previous studies (Mehdizadeh, et al., 2020; Zhai, et al., 2019). According to
391 International Commission on Microbiological Specifications for Food (ICMSF) (Gould,
392 1990), the maximum acceptable limit for fresh fish is 10^7 CFU/g. In this study, the TVC
393 of silver carp increased to 7 $\log_{10}(\text{CFU/g})$ at nearly 5 d. This indicated that silver carp
394 could not be consumed after 5-days storage, which was similar to the result of the
395 TVBN analysis. In addition, according to the European legislation (European
396 Commission, 2007), the maximum acceptable limit for raw meats is 5×10^6 CFU/g. In
397 this study, the TVC of beef increased to $\log_{10}(5 \times 10^6 \text{ CFU/g})$, namely 6.7 $\log_{10}(\text{CFU/g})$,
398 just after 4 d. This indicated that the beef sample could not be consumed after 4 d, which

399 was also similar to the result of the TVBN analysis.

400 It is generally expected that the film could indicate the meat spoilage as early as
401 possible, and the color changes are highly visible for naked eye for practical application.
402 In this study, the color differences of the film could be clearly seen after 5 days. Hence,
403 improving the gas sensitivity of the film to make the film a better indicating property
404 would be the focus of our further study.

405 **4. Conclusions**

406 LDPE-curcumin film was successfully developed through the melting extrusion
407 method. The LDPE-curcumin film, as a hydrophobic film, could prevent the leaching
408 of curcumin under high RH environment. The LDPE-curcumin film was sensitive to
409 NH₃, and a lower RH was conducive to the sensitivity. The LOD of LDPE-curcumin
410 film to NH₃ was determined to be 0.18 μM at 90% RH. The LDPE-curcumin film
411 showed yellow-to-brown color changes with the storage of silver carp and beef at 4 °C.
412 As the film is safe, low cost and suitable for industrial production, it would have a good
413 potential for application in intelligent food packaging.

414 **Declaration of competing interest**

415 None

416 **Acknowledgments**

417 The authors gratefully acknowledge the financial support provided by the National Key
418 Research and Development Program of China (2017YFC1600806, 2016YFD0401104),
419 the National Natural Science Foundation of China (31801631, 31671844, 31601543),
420 the Natural Science Foundation of Jiangsu Province (BK20160506, BE2016306,
421 BK20180865), International Science and Technology Cooperation Project of Jiangsu
422 Province (BZ2016013), the Postgraduate Research & Practice Innovation Program of
423 Jiangsu Province (KYCX17_1798), and the China Scholarship Council.

424 **References**

- 425 Cai, J., Chen, Q., Wan, X., & Zhao, J. (2011). Determination of total volatile basic nitrogen (TVB-N)
426 content and Warner-Bratzler shear force (WBSF) in pork using Fourier transform near infrared
427 (FT-NIR) spectroscopy. *Food Chemistry*, *126*(3), 1354-1360.
- 428 Chayavanich, K., Thiraphibundet, P., & Imyim, A. (2019). Biocompatible film sensors containing red
429 radish extract for meat spoilage observation. *Spectrochimica Acta Part A: Molecular and*
430 *Biomolecular Spectroscopy*, *226*, 117601-117606.
- 431 Choi, I., Lee, J. Y., Lacroix, M., & Han, J. (2017). Intelligent pH indicator film composed of agar/potato
432 starch and anthocyanin extracts from purple sweet potato. *Food Chemistry*, *218*, 122-128.
- 433 Chun, H.-N., Kim, B., & Shin, H.-S. (2014). Evaluation of a freshness indicator for quality of fish
434 products during storage. *Food Science and Biotechnology*, *23*(5), 1719-1725.
- 435 Commission, E. (2007). Commission Regulation (EC) No 1441/2007 of 5 December 2007 amending
436 Regulation (EC) No 2073/2005 on microbiological criteria for foodstuffs. *Official Journal of*
437 *the European Union*, *332*, 12-29.
- 438 Courbat, J., Briand, D., Damon-Lacoste, J., Wöllenstein, J., & de Rooij, N. F. (2009). Evaluation of pH
439 indicator-based colorimetric films for ammonia detection using optical waveguides. *Sensors*
440 *and Actuators B: Chemical*, *143*(1), 62-70.
- 441 Domínguez-Aragón, A., Olmedo-Martínez, J. A., & Zaragoza-Contreras, E. A. (2018). Colorimetric
442 sensor based on a poly(ortho-phenylenediamine-co-aniline) copolymer for the monitoring of
443 tilapia (*Oreochromis niloticus*) freshness. *Sensors and Actuators B: Chemical*, *259*, 170-176.
- 444 Dudnyk, I., Janeček, E.-R., Vaucher-Joset, J., & Stellacci, F. (2018). Edible sensors for meat and seafood
445 freshness. *Sensors and Actuators B: Chemical*, *259*, 1108-1112.
- 446 Esatbeyoglu, T., Ulbrich, K., Rehberg, C., Rohn, S., & Rimbach, G. (2015). Thermal stability, antioxidant,
447 and anti-inflammatory activity of curcumin and its degradation product 4-vinyl guaiacol. *Food*
448 *& Function*, *6*(3), 887-893.
- 449 Ezati, P., Tajik, H., & Moradi, M. (2019). Fabrication and characterization of alizarin colorimetric
450 indicator based on cellulose-chitosan to monitor the freshness of minced beef. *Sensors and*
451 *Actuators B: Chemical*, *285*, 519-528.
- 452 Gould, G. (1990). Micro-organisms in foods 2. Sampling for microbiological analysis: Principles and
453 specific applications: ICMSF, Blackwell Scientific Publications, London, 1986, 2nd Edn, 293
454 pp., ISBN 0-632-01567-5.
- 455 Huang, L., Zhao, J., Chen, Q., & Zhang, Y. (2013). Rapid detection of total viable count (TVC) in pork
456 meat by hyperspectral imaging. *Food Research International*, *54*(1), 821-828.
- 457 Huang, S., Xiong, Y., Zou, Y., Dong, Q., Ding, F., Liu, X., & Li, H. (2019). A novel colorimetric indicator
458 based on agar incorporated with *Arnebia euchroma* root extracts for monitoring fish freshness.
459 *Food Hydrocolloids*, *90*, 198-205.
- 460 Jia, R., Tian, W., Bai, H., Zhang, J., Wang, S., & Zhang, J. (2019). Amine-responsive cellulose-based
461 ratiometric fluorescent materials for real-time and visual detection of shrimp and crab freshness.
462 *Nature Communications*, *10*(1), 795-802.
- 463 Kachele, R., Zhang, M., Gao, Z., & Adhikari, B. (2017). Effect of vacuum packaging on the shelf-life of
464 silver carp (*Hypophthalmichthys molitrix*) fillets stored at 4 °C. *Lwt-Food Science and*
465 *Technology*, *80*, 163-168.
- 466 Karim, F., Hijaz, F., Kastner, C. L., & Smith, J. S. (2011). Ammonia gas permeability of meat packaging

467 materials. *Journal of Food Science*, 76(2), T59-64.

468 Khattab, T. A., Dacrory, S., Abou-Yousef, H., & Kamel, S. (2019). Development of microporous
469 cellulose-based smart xerogel reversible sensor via freeze drying for naked-eye detection of
470 ammonia gas. *Carbohydrate Polymers*, 210, 196-203.

471 Koskela, J., Sarfraz, J., Ihalainen, P., Määttänen, A., Pulkkinen, P., Tenhu, H., Nieminen, T., Kilpelä, A.,
472 & Peltonen, J. (2015). Monitoring the quality of raw poultry by detecting hydrogen sulfide with
473 printed sensors. *Sensors and Actuators B: Chemical*, 218, 89-96.

474 Kotha, R. R., & Luthria, D. L. (2019). Curcumin: biological, pharmaceutical, nutraceutical, and
475 analytical aspects. *Molecules*, 24(16).

476 Kuswandi, B., Jayus, Larasati, T. S., Abdullah, A., & Heng, L. Y. (2011). Real-time monitoring of shrimp
477 spoilage using on-package sticker sensor based on natural dye of curcumin. *Food Analytical
478 Methods*, 5(4), 881-889.

479 Kuswandi, B., Jayus, Restyana, A., Abdullah, A., Heng, L. Y., & Ahmad, M. (2012). A novel colorimetric
480 food package label for fish spoilage based on polyaniline film. *Food Control*, 25(1), 184-189.

481 Lee, K., Baek, S., Kim, D., & Seo, J. (2019). A freshness indicator for monitoring chicken-breast spoilage
482 using a Tyvek® sheet and RGB color analysis. *Food Packaging and Shelf Life*, 19, 40-46.

483 Lee, S. J., & Rahman, A. T. M. M. (2014). Chapter 8 - Intelligent packaging for food products. In J. H.
484 Han (Ed.), *Innovations in Food Packaging (Second Edition)* (pp. 171-209). San Diego:
485 Academic Press.

486 Lin, T., Wu, Y., Li, Z., Song, Z., Guo, L., & Fu, F. (2016). Visual monitoring of food spoilage based on
487 hydrolysis-induced silver metallization of Au nanorods. *Analytical Chemistry*, 88(22), 11022-
488 11027.

489 Liu, J., Wang, H., Guo, M., Li, L., Chen, M., Jiang, S., Li, X., & Jiang, S. (2019). Extract from *Lycium
490 ruthenicum Murr.* incorporating κ -carrageenan colorimetric film with a wide pH-sensing range
491 for food freshness monitoring. *Food Hydrocolloids*, 94, 1-10.

492 Liu, J., Wang, H., Wang, P., Guo, M., Jiang, S., Li, X., & Jiang, S. (2018). Films based on κ -carrageenan
493 incorporated with curcumin for freshness monitoring. *Food Hydrocolloids*, 83, 134-142.

494 Long, L., Cao, S., Jin, B., Yuan, X., Han, Y., & Wang, K. (2019). Construction of a novel fluorescent
495 probe for on-site measuring hydrogen sulfide levels in food samples. *Food Analytical Methods*,
496 12(4), 852-858.

497 Luo, X., & Lim, L.-T. (2020). Curcumin-loaded electrospun nonwoven as a colorimetric indicator for
498 volatile amines. *Lwt-Food Science and Technology*, 128, 109493-109503.

499 Ma, Q., Du, L., & Wang, L. (2017). Tara gum/polyvinyl alcohol-based colorimetric NH₃ indicator films
500 incorporating curcumin for intelligent packaging. *Sensors and Actuators B: Chemical*, 244, 759-
501 766.

502 Ma, Q., & Wang, L. (2016). Preparation of a visual pH-sensing film based on tara gum incorporating
503 cellulose and extracts from grape skins. *Sensors and Actuators B: Chemical*, 235, 401-407.

504 Ma, Z., Chen, P., Cheng, W., Yan, K., Pan, L., Shi, Y., & Yu, G. (2018). Highly sensitive, printable
505 nanostructured conductive polymer wireless sensor for food spoilage detection. *Nano Letters*,
506 18(7), 4570-4575.

507 Mehdizadeh, T., Tajik, H., Langroodi, A. M., Molaei, R., & Mahmoudian, A. (2020). Chitosan-starch
508 film containing pomegranate peel extract and *Thymus kotschyanus* essential oil can prolong the
509 shelf life of beef. *Meat Science*, 163, 108073-108083.

510 Mills, A., Wild, L., & Chang, Q. (1995). Plastic colorimetric film sensors for gaseous ammonia.

511 *Microchimica Acta*, 121(1-4), 225-236.

512 Mo, R., Quan, Q., Li, T., Yuan, Q., Su, T., Yan, X., Qian, Z. J., Hong, P., Zhou, C., & Li, C. (2017). An
513 intelligent label for freshness of fish based on a porous anodic aluminum membrane and
514 bromocresol green. *ChemistrySelect*, 2(28), 8779-8784.

515 Pacquit, A., Frisby, J., Diamond, D., Lau, K. T., Farrell, A., Quilty, B., & Diamond, D. (2007).
516 Development of a smart packaging for the monitoring of fish spoilage. *Food Chemistry*, 102(2),
517 466-470.

518 Pacquit, A., Lau, K. T., McLaughlin, H., Frisby, J., Quilty, B., & Diamond, D. (2006). Development of a
519 volatile amine sensor for the monitoring of fish spoilage. *Talanta*, 69(2), 515-520.

520 Pourreza, N., & Golmohammadi, H. (2015). Application of curcumin nanoparticles in a lab-on-paper
521 device as a simple and green pH probe. *Talanta*, 131, 136-141.

522 Priyadarsini, K. I. (2014). The chemistry of curcumin: from extraction to therapeutic agent. *Molecules*,
523 19(12), 20091-20112.

524 Qin, Y., Liu, Y., Zhang, X., & Liu, J. (2020). Development of active and intelligent packaging by
525 incorporating betalains from red pitaya (*Hylocereus polyrhizus*) peel into starch/polyvinyl
526 alcohol films. *Food Hydrocolloids*, 100, 105410.

527 Saliu, F., & Della Pergola, R. (2018). Carbon dioxide colorimetric indicators for food packaging
528 application: applicability of anthocyanin and poly-lysine mixtures. *Sensors and Actuators B:
529 Chemical*, 258, 1117-1124.

530 Tønnesen, H. H., Karlsen, J., & van Henegouwen, G. B. (1986). Studies on curcumin and curcuminoids
531 VIII. Photochemical stability of curcumin. *Zeitschrift für Lebensmittel-Untersuchung und
532 Forschung*, 183(2), 116-122.

533 Wang, Y. C., Lu, L., & Gunasekaran, S. (2017). Biopolymer/gold nanoparticles composite plasmonic
534 thermal history indicator to monitor quality and safety of perishable bioproducts. *Biosensors
535 and Bioelectronics*, 92, 109-116.

536 Wells, N., Yusufu, D., & Mills, A. (2019). Colourimetric plastic film indicator for the detection of the
537 volatile basic nitrogen compounds associated with fish spoilage. *Talanta*, 194, 830-836.

538 Xiang, H., Sun-Waterhouse, D., Cui, C., Wang, W., & Dong, K. (2018). Modification of soy protein
539 isolate by glutaminase for nanocomplexation with curcumin. *Food Chemistry*, 268, 504-512.

540 Zhai, X., Li, Z., Shi, J., Huang, X., Sun, Z., Zhang, D., Zou, X., Sun, Y., Zhang, J., Holmes, M., Gong,
541 Y., Povey, M., & Wang, S. (2019). A colorimetric hydrogen sulfide sensor based on gellan gum-
542 silver nanoparticles bionanocomposite for monitoring of meat spoilage in intelligent packaging.
543 *Food Chemistry*, 290, 135-143.

544 Zhai, X., Li, Z., Zhang, J., Shi, J., Zou, X., Huang, X., Zhang, D., Sun, Y., Yang, Z., Holmes, M., Gong,
545 Y., & Povey, M. (2018). Natural biomaterial-based edible and pH-sensitive films combined with
546 electrochemical writing for intelligent food packaging. *Journal of Agricultural and Food
547 Chemistry*, 66(48), 12836-12846.

548 Zhai, X., Shi, J., Zou, X., Wang, S., Jiang, C., Zhang, J., Huang, X., Zhang, W., & Holmes, M. (2017).
549 Novel colorimetric films based on starch/polyvinyl alcohol incorporated with roselle
550 anthocyanins for fish freshness monitoring. *Food Hydrocolloids*, 69, 308-317.

551 Zhai, X., Zou, X., Shi, J., Huang, X., Sun, Z., Li, Z., Sun, Y., Li, Y., Wang, X., Holmes, M., Gong, Y.,
552 Povey, M., & Xiao, J. (2020). Amine-responsive bilayer films with improved illumination
553 stability and electrochemical writing property for visual monitoring of meat spoilage. *Sensors
554 and Actuators B: Chemical*, 302, 127130-127141.

555 Zhang, C., Yin, A.-X., Jiang, R., Rong, J., Dong, L., Zhao, T., Sun, L.-D., Wang, J., Chen, X., & Yan, C.-
556 H. (2013). Time-temperature indicator for perishable products based on kinetically
557 programmable Ag overgrowth on Au nanorods. *ACS Nano*, 7(5), 4561-4568.

558 Zhang, J., Zou, X., Zhai, X., Huang, X., Jiang, C., & Holmes, M. (2019). Preparation of an intelligent
559 pH film based on biodegradable polymers and roselle anthocyanins for monitoring pork
560 freshness. *Food Chemistry*, 272, 306-312.

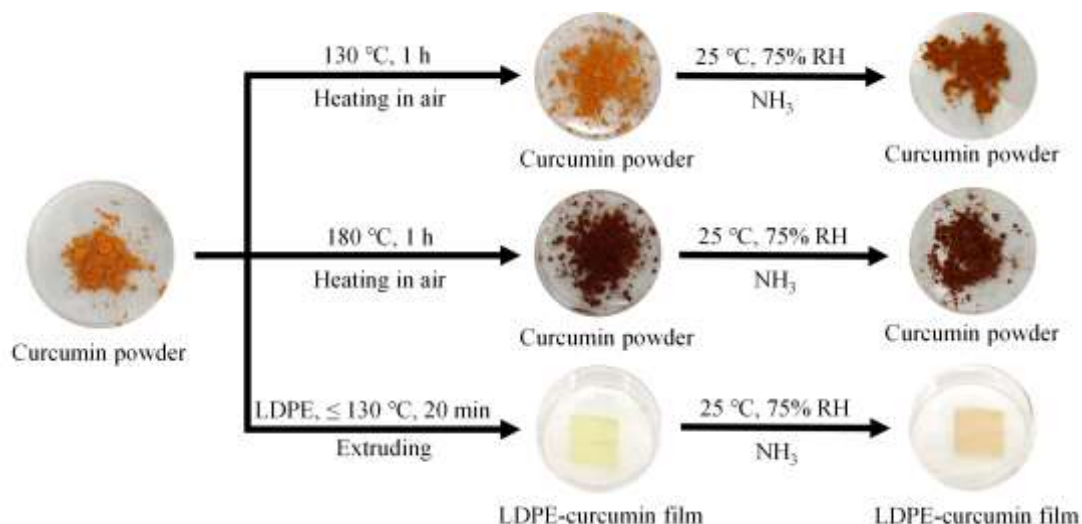
561 Zhang, X., Lu, S., & Chen, X. (2014). A visual pH sensing film using natural dyes from *Bauhinia*
562 *blakeana* Dunn. *Sensors and Actuators B: Chemical*, 198, 268-273.

563 Zhu, R., Desroches, M., Yoon, B., & Swager, T. M. (2017). Wireless oxygen sensors enabled by Fe(II)-
564 polymer wrapped carbon nanotubes. *ACS Sensors*, 2(7), 1044-1050.

565 Zia, J., Paul, U. C., Heredia-Guerrero, J. A., Athanassiou, A., & Fragouli, D. (2019). Low-density
566 polyethylene/curcumin melt extruded composites with enhanced water vapor barrier and
567 antioxidant properties for active food packaging. *Polymer*, 175, 137-145.

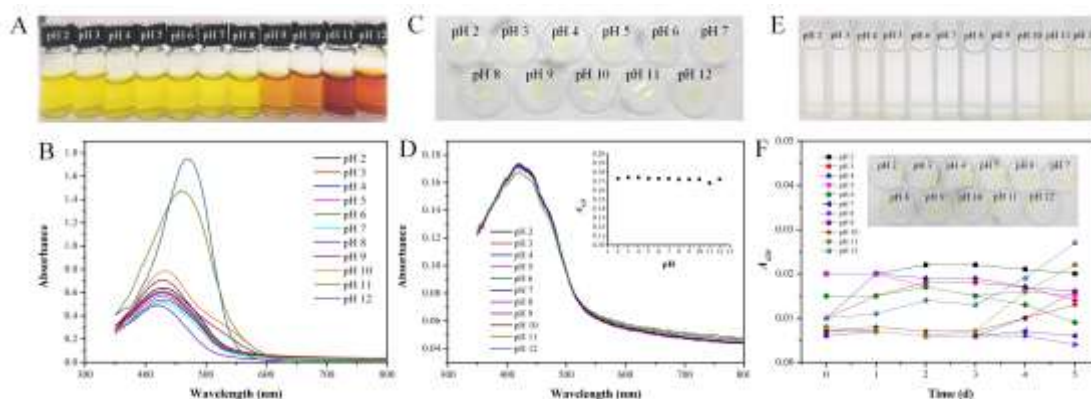
568

569



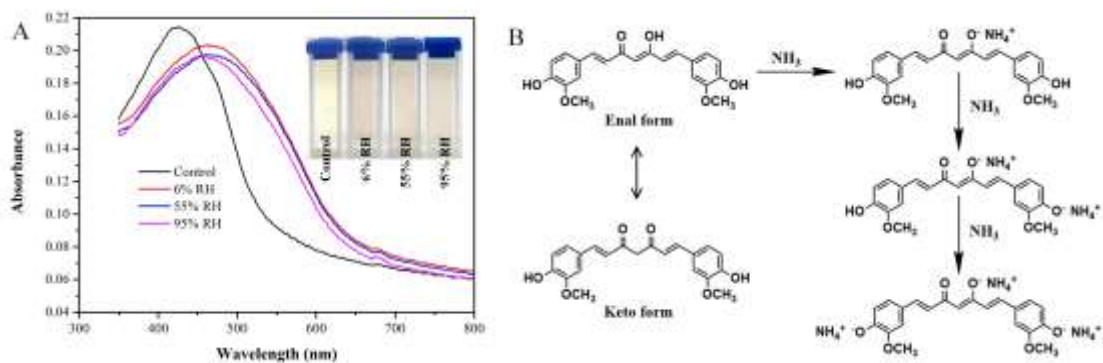
570
571
572
573
574
575
576
577
578

Fig. 1. The photos of curcumin powder and LDPE-curcumin film.



579
580
581
582
583
584
585
586

Fig. 2. (A) The photos and (B) UV-Vis spectra of curcumin solution at pH 2-12. (C) The photos and (D) UV-Vis spectra of LDPE-curcumin film immersed in buffer solutions, and inset of (D) is the A_{420} of the film immersed in buffer solution. (E) The photos and (F) A_{420} of lixiviums of LDPE-curcumin film immersed in buffer solution, and inset of (F) is the photo of LDPE-curcumin film after immersed in buffer solution for 5 d.

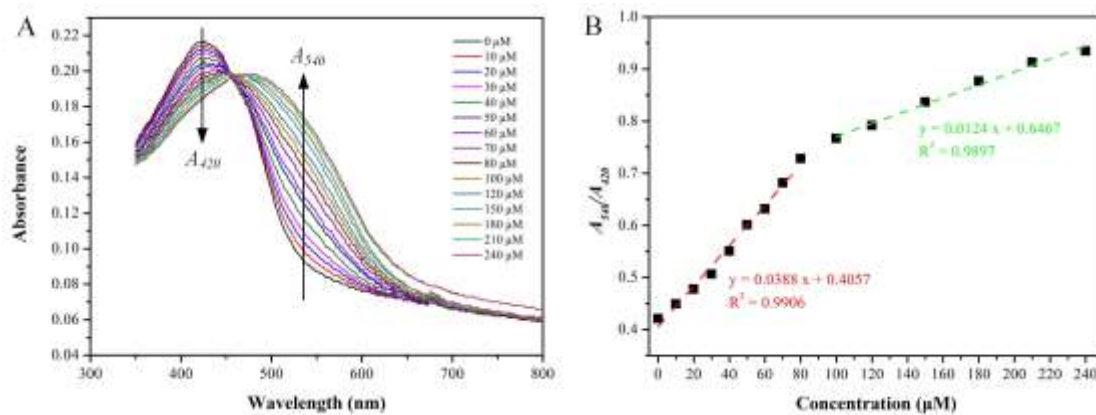


587

588 Fig. 3. (A) UV-Vis spectra and photos (inset) of LDPE-curcumin film after exposed to 200 μM of
 589 NH_3 , and (B) the proposed reaction mechanism between curcumin and NH_3

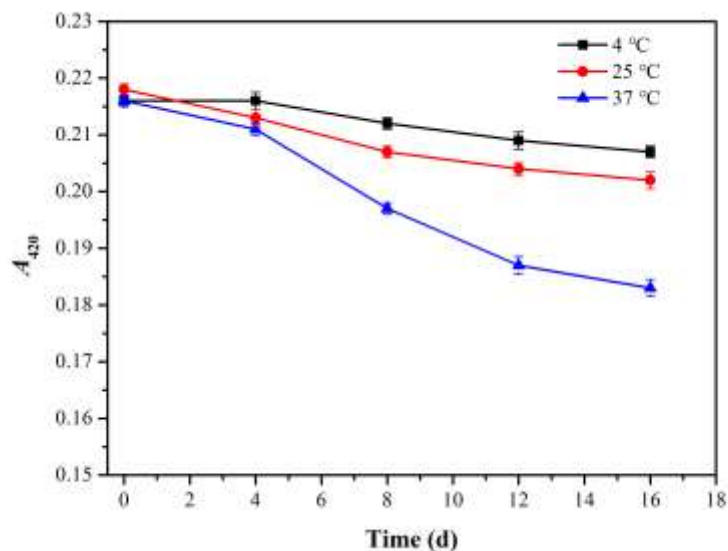
590

591



592

593 Fig. 4. (A) The UV-Vis spectra and (B) A_{540}/A_{420} of LDPE-curcumin film in response to NH_3 with
 594 concentrations of 0-240 μM .

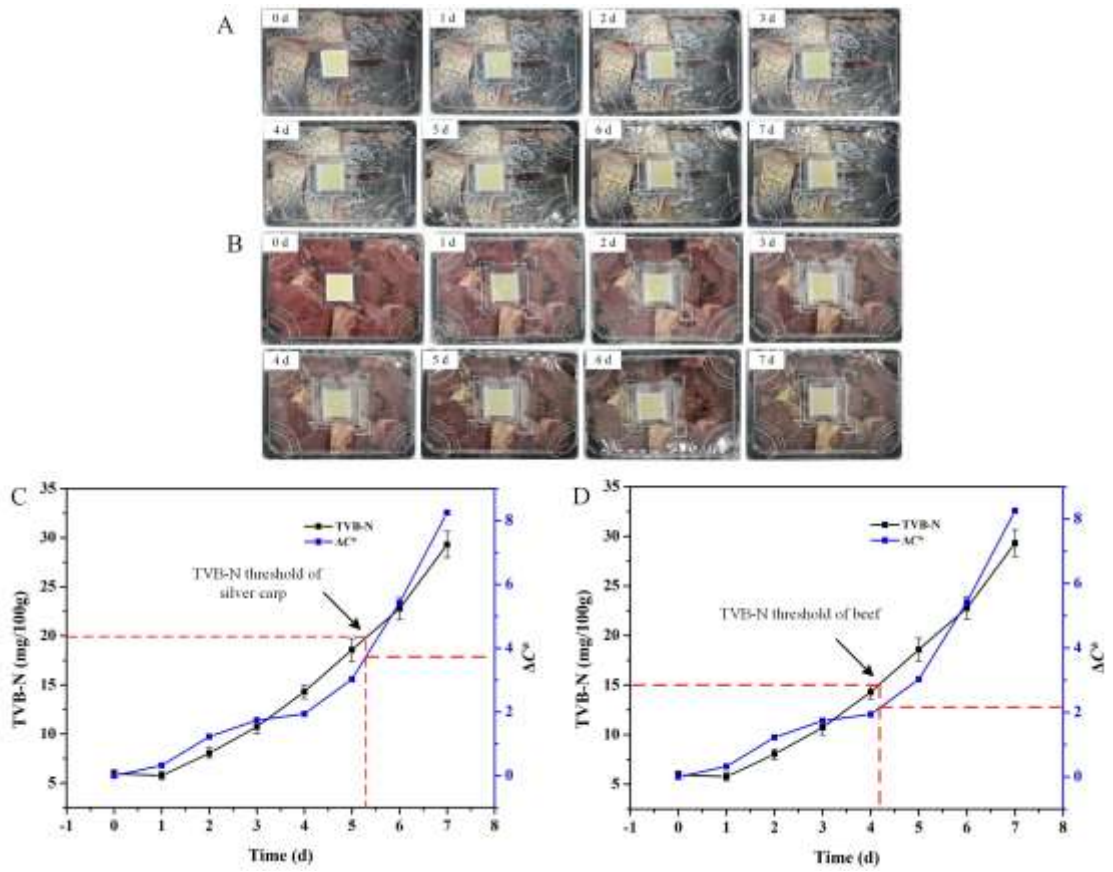


595

596 Fig. 5. The changes of A_{420} of the LDPE-curcumin film stored at 4, 25 and 37 $^{\circ}\text{C}$.

597

598



599

600 Fig. 6. The photos of the packages with (A) silver carp and (B) beef, and the relation between TVB-
 601 N and ΔC^* of LDPE-curcumin film for (C) silver carp and (D) beef.

602

603

604

605

606